Hindawi
Scientific Programming
Volume 2021, Article ID 1911381, 8 pages
https://doi.org/10.1155/2021/1911381

Research Article

Deep Learning in Laparoscopic Colorectal Carcinoma Surgery under Magnetic Resonance Imaging

Shuguang Pan, Wei Tang, Tiejun Zhou, and Wei Luo

Department of Colorectal Surgery, Hunan Cancer Hospital, Changsha 410013, Hunan, China

Correspondence should be addressed to Wei Luo; luowei@hnca.org.cn

Received 12 May 2021; Revised 19 June 2021; Accepted 1 July 2021; Published 13 July 2021

Academic Editor: Gustavo Ramirez

This study aimed to explore the application effect of magnetic resonance imaging (MRI) based on deep learning in laparoscopic surgery for colorectal carcinoma (CRC). 40 patients with CRC who were diagnosed and required laparoscopic surgery were selected in the research. The MRI scan images of all patients were processed based on the convolutional neural network algorithm. The MRI images before and after treatment were set as the control group and the experimental group, respectively. The consistency of MRI results with laparoscopic and postoperative pathological biopsy results was observed. Through the comparative analysis of the research results, in terms of consistency with the surgical plane, the assessment results of the experimental group were more consistent than those of the control group and direct observation under laparoscopy, and the difference was statistically significant ($P < 0.05$). In terms of tumor T staging, the consistency between the experimental group and pathological biopsy results was superior to that of the control group, with considerable difference ($P < 0.05$). In conclusion, practically speaking, the application of MR images based on convolutional neural network algorithm in laparoscopic CRC surgery was better than conventional MRI technology. However, the research was a small-scale pathological study, which was not very representative.

1. Introduction

Due to the changes in people's living and eating habits and the current situation of the aging population in China, colorectal carcinoma (CRC) becomes a very common gastrointestinal cancer in China. The incidence of this disease is increasing year by year [1], which has brought great threat to people's life and health.

According to statistical analysis, most patients in China are already in the middle and advanced stages of cancer when they are diagnosed [2]. At present, the main treatment method for CRC is surgical resection. To reduce the probability of local recurrence after surgery, total mesorectal excision (TME) has been proposed and recognized by most scholars, and more and more scholars believe that it is the gold standard for radical resection of rectal carcinoma [3]. Later, with the development of laparoscopic technology, this technology and TME were combined by people and applied to the surgical treatment of CRC and achieved good therapeutic effects. Compared with traditional open surgery, CRC surgery under laparoscopy has a minimally invasive effect and less bleeding. It can recover fast after the operation, and the treatment effect of the two methods is the same [4]. Therefore, TEM has good clinical application value and has been widely recognized. However, this technology displays two-dimensional pictures based on the laparoscope. The precise and meticulous operation in the fascial space between the intestines lacks intuitiveness and authenticity. It is easy to locate incorrectly and cause other tissue damages [5]. Therefore, it is very important to construct the surgical plane of the intestinal fascial space before surgery. The tumor and its mesangial membrane can be completely removed by following this surgical plane, and the adjacent organs, blood vessels, and autonomic nerve plexus in the pelvic cavity can be avoided as much as possible [6]. Shinohara et al. [7] studied and analyzed embryological and anatomical theories similar to TME in 2009 and published the concept and technique of complete mesocolic excision (CME). It

provided the correct anatomical level and surgical approach for the reasonable operation of colon cancer. In recent years, with the continuous progress of magnetic resonance imaging (MRI) technology, it has also become the main imaging examination method for the preoperative evaluation of malignant tumors. MRI sequence images are deemed as evidence for tumor staging by showing the depth of invasion of colorectal cancer tumors and the invasion of surrounding tissues or organs. However, the clarity of the image displayed after MRI scan is different for colorectal cancer at different stages of the disease. For example, MRI can show good resolution for T3 and T4 carcinomas, but cannot provide accurate display for T1 and T2 [8, 9].

Deep learning artificial intelligence was used to optimize MRI technology and applied to the examination of patients. The location, staging, and appropriate postoperative path of the lesion were determined based on the image, and the therapeutic effect of laparoscopic CRC surgery was studied under the guidance of MR imaging technology based on deep learning.

2. Methods

2.1. Research Object. 40 patients with CRC who were diagnosed and required laparoscopic surgery were selected in the research from September 2019 to March 2020. All patients were checked for blood routine, biochemical, tumor indicators, electrocardiogram, and MRI scan of the diseased location before surgery. Among them, there were 23 male patients and 17 female patients. All patients ranged in age from 50 to 72 years, with an average age of 62 ± 3.2 years. The MRI scan images of all patients were processed based on deep learning, and the MRI images before and after the processing were set as the control group and the experimental group.

Inclusion criteria were as follows: (i) patients diagnosed with CRC by colonoscopy and pathological biopsy; the diagnosis result was in accordance with the AJCC seventh edition TNM staging standard [10], as shown in Figure 1; (ii) patients with the TNM staging range: T: −4, N: 0–2, and M: 0 by preoperative MRI scan and ultrasound endoscopy; (iii) all patients were over 18 years old and under 75 years old; (iv) patients without severe damage to the heart, lungs, liver, kidneys, and other organs; (v) the patients were informed of the research content, and patient's consent was obtained.

Exclusion criteria were as follows: (i) patients with tumors and intestinal obstruction; (ii) patients whose cancer lesions had metastasized far away; (iii) patients with previous abdominal surgery and who were not suitable for laparoscopy; (iv) patients with a previous history of radiotherapy and chemotherapy; (v) patients with cancerous diseases that accompany other organs. This study had been approved by the ethics committee of the hospital, and all subjects included in the study had signed informed consent.

2.2. Research Methods

2.2.1. MRI Scan Method. All patients cannot eat within 4–6 hours the day before the preoperative MRI abdominal scan, the intestines were cleaned, and there was no urine excretion one hour prior to the scan. There was one more check for female patients that was whether the intrauterine contraceptive device in the uterus was removed. Ten minutes before the MRI scan, 10 mg of 654-2 and 200–300 mL of 70% NaCl solution needed to be injected from the patient's anus to the colorectal. The operation process of the examination is shown in Figure 2. VSTIA was used to reconstruct the disease sites of the original data at multiple levels, and the relationship between lymph nodes and blood vessels was shown in multiple directions. The imaging evaluation criteria of the colorectal surgical plane under reconstruction were observed, and the tumor staging of the patients was conducted. Then, the corresponding laparoscopic surgical access and surgical methods were customized, and the laparoscopic surgical access during the operation was observed.

2.2.2. MR Imaging Technology Based on Deep Learning. The convolutional neural network algorithm was used in the research to optimize the MRI technology. The algorithm process is as follows.

After MRI was input, the characteristics of the MRI image output after the operation of the convolution algorithm were expressed as follows:

$$F_j^j = f\left(\sum_{i \in M_j} F_i^{l-1} * P_{ij}^1 + b_j^l\right). \tag{1}$$

In equation (1), l refers to the current layer, M_j refers to the set of all the inputted MRI feature images, and b refers to the bias corresponding to the MRI output feature images. The weight of the BP algorithm was used as an improvement and was expressed as equations (2) and (3):

$$\frac{\alpha G}{\alpha p^l} = x^{l-1}\left(\gamma^l\right)^T, \tag{2}$$

$$\nabla p^l = -\lambda\left(\frac{\alpha G}{\alpha p^l}\right). \tag{3}$$

To make the scale of the MRI feature map of the convolutional layer and the pooling layer the same, the difference between the pooling layer and the convolutional layer was sampled during the establishment process, and the corresponding error was obtained. Then, the final gradient was obtained by multiplying the partial derivative of the image feature map of the convolutional layer MRI. The weights of MRI feature maps were shared in the pooling layer, and the shared value was χ. The calculation of the

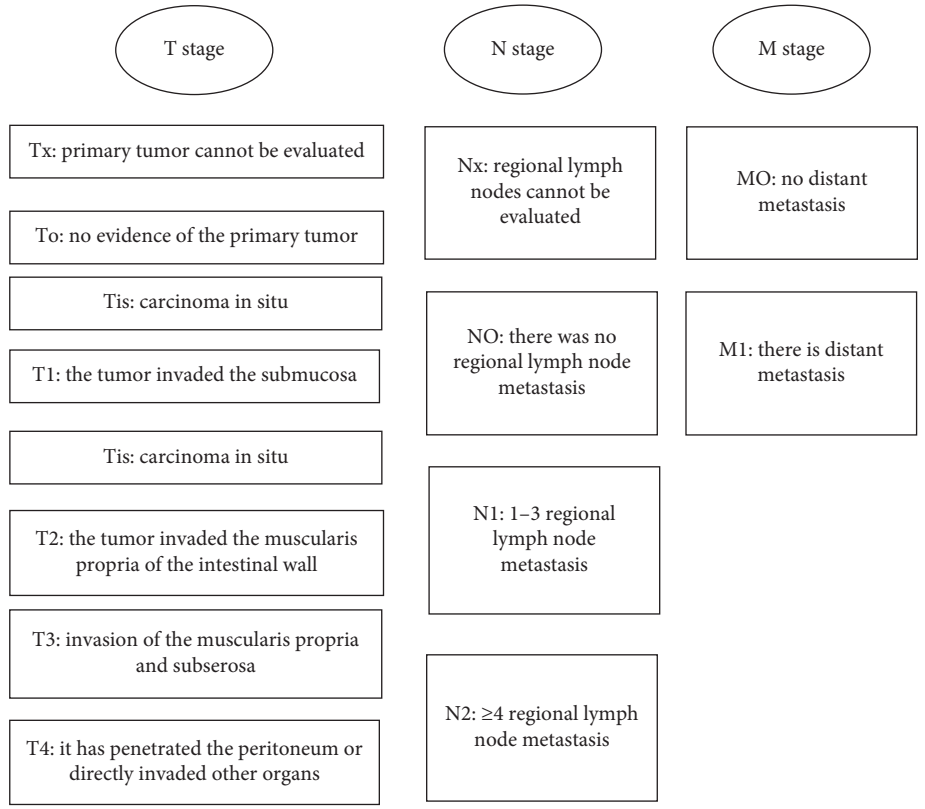

Figure 1: AJCC seventh edition TNM staging standard.

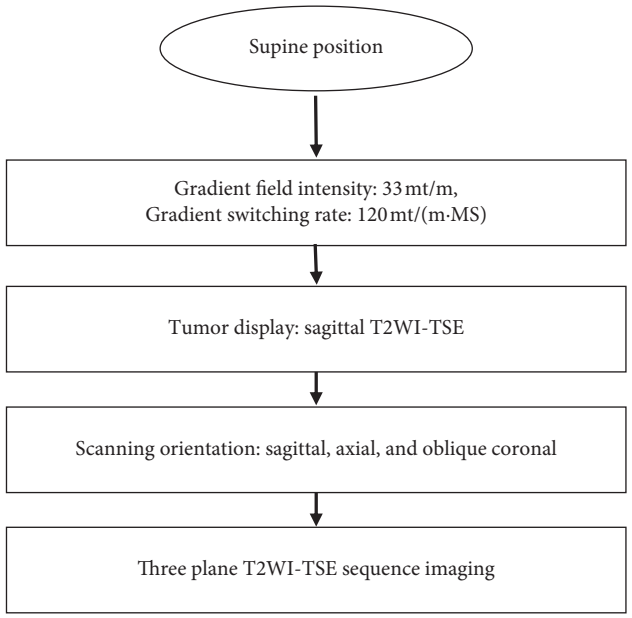

Figure 2: MRI scanning process.

gradient of the convolutional layer was shown as equations (4) and (5):

$$\alpha_j^l = \chi_j^{l+1}\left(f'\left(u_j^l\right) \circ uq\left(\gamma_j^{l+1}\right)\right), \tag{4}$$

$$u_j^l = p_j^l F_j^{l-1} + b_j^l. \tag{5}$$

In the above equation, $uq(\cdot)$ refers to the sampling operation in the previous step, and the gradient of the given feature graph was calculated. After the calculation of the weight was completed, according to bias gradient equation (6) in the BP algorithm, the bias gradient of each feature map in layer l was calculated.

$$\frac{\alpha G}{\alpha b} = \gamma_l. \tag{6}$$

The gradient of bias b can be obtained by summation of the errors of all nodes in each feature graph, as shown in the following equation:

$$\frac{\alpha G}{\alpha b} = \sum_{u,v}\left(\gamma_j^l\right)_{u,v}. \tag{7}$$

The number of MRI feature maps of the pooling layer and the convolutional layer was the same; only the size of the MRI feature map was different. The MRI feature map output by the pooling layer was expressed as the following equation:

$$F_j^l = f\left(\chi_j^l \operatorname{down}\left(F_j^{l-1}\right) + b_j^l\right). \tag{8}$$

In (8), down $(\cdot)$ refers to the error sampling function of the next layer, χ refers to the weight of the pooling layer, and b represents the bias of the pooling layer.

To obtain the parameters of the pooling layer, the gradient of weight and bias are needed to be calculated first, which was classified into two situations. The first type: the error of the pooling layer was calculated by BP algorithm when the pooling layer was directly connected to the full connection layer. The second type: the pooling layer was connected with the convolutional layer; the calculation of the gradient of bias b and the convolutional layer was the same as that of equation (7). The gradient calculation of the weight γ was as follows:

$$\frac{\alpha G}{\alpha \chi_j^l} = \sum_{u,v} \left(\gamma_j^l \circ d_j^l\right)_{u,v}. \tag{9}$$

In addition, in (10), the gradient equation was used to update the weight and bias:

$$d_j^l = \operatorname{down}\left(F_j^{l-1}\right). \tag{10}$$

The calculation and processing procedure of MRI images of CRC using convolutional neural network algorithm is shown in Figure 3.

2.3. Observation Indicators.

(a) The degree of consistency between the surgical plane reconstructed by the MRI technique before and after optimization and the surgical plane photographed under laparoscopy was observed, and whether the tumor invaded Toldt's line was observed (Toldt's line: the linear shadow composed of the ascending and descending posterior lobe of the mesocolon and anterior renal fascia [11])

(b) The results of postoperative biopsy and MRI examination before and after optimization were compared

2.4. Statistical Methods. SPSS 22.0 statistical software system was used for data entry, sorting, and statistical analysis. The difference of count data adopted X^2 test, and the difference of measurement data adopted t-test. The difference of multiple-sample means was analyzed by variance analysis. LSD method was used when the variance was uniform, and Dunnett T3 method was used when the variance was uneven. $P < 0.05$ was statistically different. The kappa test was performed on the consistency between the surgical plane displayed by the preoperative image and the intraoperative findings. When kappa > 0.75, the consistency between the two was strong, when $0.4 \leq$ kappa < 0.75, the consistency between the two was general, and when kappa < 0.4, the consistency between the two was poor.

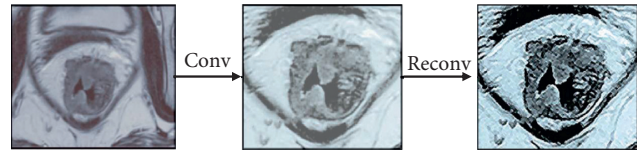

Figure 3: Convolutional neural network algorithm processing procedure of rectal cancer MRI images.

3. Results

3.1. Difference of MRI Results of the Control Group. Figure 4 shows the staging of MRI images based on the patient's postoperative pathological biopsy. The MRI images of each stage of the tumor were observed. It was found that the T1 and T2 tumors invaded the layer of the intestinal wall that was not discernible, but it was impossible to observe whether the mucosal layer or the intrinsic layer was invaded by the tumor. However, the T3 and T4 phases can be distinguished. Figure 5 shows that the surgical plane reconstructed under laparoscopic and MRI images of the control group was compared, and it was found that accurate consistency judgment could not be made.

3.2. Difference of the Results of MRI Examination in the Experimental Group. Figures 6 and 7 show optimized MRI images based on Figures 4 and 5, and they were compared with the images in Section 3.1. The optimized MRI images of each stage of the tumor were observed. It was found clearly that MRI images of T1 and T2 tumor stages cannot be differentiated, and it is also indistinguishable whether the mucosal layer or the basal layer propria was invaded by the tumor. However, the T3 and T4 tumor stages can be clearly distinguished. Figure 7 shows the surgical plane difference between laparoscopic and MRI image reconstruction in the experimental group, and it was found that the degree of agreement assessed was about 87%. The probability was high, but this was only one case, and it was not representative.

3.3. Difference between Results under Laparoscopy and MRI Images. The MRI image data of the two groups and the tumor invasion under laparoscopy were statistically sorted according to whether Toldt's line was invaded or not, as shown in Table 1. Through comparative analysis, it was found that the consistency between the control group and the laparoscopic results was $0.4 \leq$ kappa < 0.75, which meant that the consistency between the two was general, as shown in Figure 8. The consistency difference between the experimental group and the laparoscopy results was kappa > 0.75, which indicated that the results of the two had a strong consistency, as shown in Figure 9. It was concluded that the result of tumor invasion of Toldt's line in the experimental group was closer to the situation observed under laparoscopy than the result obtained in the control group, with considerable difference ($P < 0.05$).

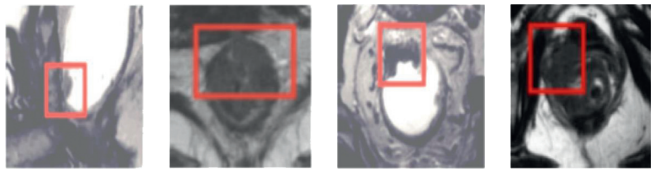

(a) (b) (c) (d)

Figure 4: Difference of images of tumors in each stage after MRI examination in the control group (red boxes indicate the tumor sites). (a) T1. (b) T2. (c) T3. (d) T4.

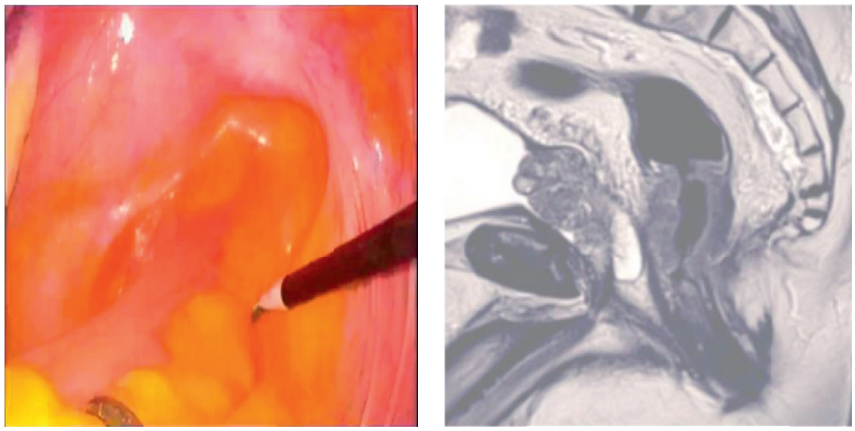

(a) (b)

Figure 5: Difference of surgical planes reconstructed by laparoscopic and MRI images in the control group.

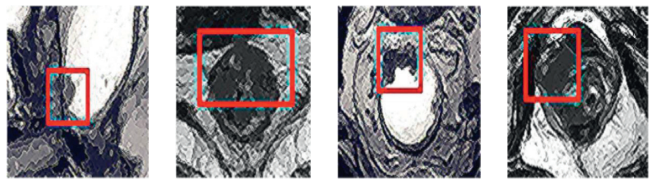

(a) (b) (c) (d)

Figure 6: Difference of the images of tumors in each stage after MRI examination in the experimental group (red boxes indicate the tumor sites). (a) T1. (b) T2. (c) T3. (d) T4.

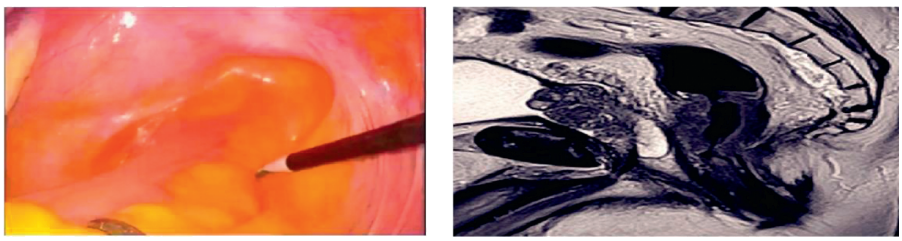

(a) (b)

Figure 7: Difference of surgical planes reconstructed by laparoscopic and MRI images in the experimental group.

3.4. Difference between Laparoscopic Results and MRI Results. The MRI image data of the two groups and tumor T staging under pathological biopsy were statistically sorted out, as shown in Table 2. Through comparative analysis, it was found that the consistency of T staging and pathological biopsy results in the control group was $0.4 \leq \text{kappa} < 0.75$,

Table 1: Difference of the MRI image and laparoscopic tumor invasion of Toldt's line.

Group range	MRI		Laparoscopy
	The control group	The experimental group	
Infringe	26	32	36
Not infringe	14	8	4

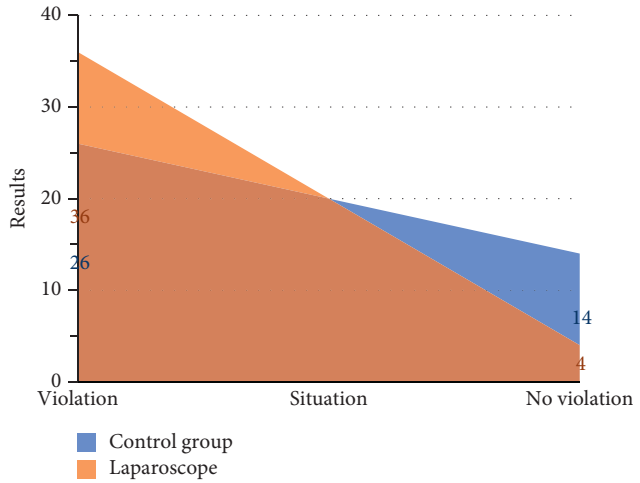

Figure 8: Difference of consistency between the control group and laparoscopy results.

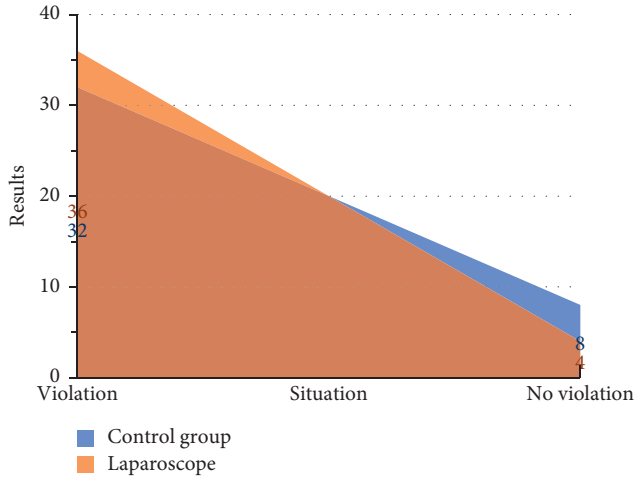

Figure 9: Difference of consistency between the experimental group and laparoscopic results.

which meant that the consistency between the two was general. The consistency of T staging and pathological biopsy results in the experimental group was kappa > 0.75, which indicated that the results of the two had a strong consistency. After the consistency between the two groups was compared, the results of T staging in the experimental group were closer to those observed by pathological biopsy than those in the control group, and the difference was great ($P < 0.05$).

Table 2: Statistical difference of T staging results of CRC tumors in the three groups.

	MRI		The pathological biopsy
	The control group	The experimental group	
T1	19	16	12
T2	9	12	16
T3	8	9	9
T4	4	3	3

4. Discussion

To reduce the recurrence rate of postoperative local lesions of patients with advanced CRC, Bahadoer et al. [12] and Shinohara et al. [7] put forward TME and CME based on embryology theory in 1982 and 2009, respectively, both of which proposed reasonable and effective anatomical theories and surgical pathways for CRC surgery. Birbeck et al. [13] studied 608 patients with rectal cancer and found that CRM can not only reduce the probability of local recurrence of CRC but also was a strong predictor of the overall survival rate of patients. The two surgical methods TME and CME focus on accurately separating the anatomical plane between the visceral layer and the parietal fascia so that the complete mesorectal membrane was separated [14, 15]. The requirements of laparoscopic surgery were very detailed, so it was necessary to evaluate CRC before surgery. The MRI technology was used in the research to observe and evaluate the situation around CRC lesions through three-dimensional reconstruction of the abdominal anatomical plane, and a good effect was obtained. There were many methods for the preoperative evaluation of CRC, but the main inspection techniques were MRI, CT, and ultrasound. The intracavitary ultrasound probe directly contacted with the intestinal wall during inspection, and the internal conditions of the intestinal wall were clearly displayed. In the evaluation of tumor T staging, the intracavitary ultrasound probe had certain advantages over MRI, CT, and other imaging techniques, but there were many interfering factors. It is difficult to repeat the examination, and the overall anatomical plane was not as intuitive as MRI and CT images [16, 17]. Although CT was simple in operation, it was basically the same as MRI in the display of tumor staging. It can distinguish T3 and T4 tumors, but cannot accurately distinguish T1 and T2 tumors [18]. As for the MRI technology, with the continuous development of the technology, it had been well improved, and it played an important role in the preoperative evaluation of malignant tumors. The accuracy of T staging for CRC tumors was also high, which had gradually approached the accuracy of intracavitary ultrasound diagnosis [8]. The application of imaging techniques in the preoperative evaluation of CRC has attracted many experts' and scholars' attention, and these experts and scholars have carried out a lot of analyses and research studies on it. Zhang et al. [19] used the MSCTA 3D reconstruction technology in the treatment of CRC. The consistency between the 3D reconstruction of MSCTA and the actual surgical plane was compared, and the kappa

consistency test $K = 0.769$ was obtained between the two, which proved that the 3D reconstruction of MSCTA had a good effect in guiding the treatment of laparoscopic CRC. Bian et al. [20] also studied and analyzed the clinical guiding significance of MSCTA three-dimensional reconstruction for laparoscopic CRC radical resection. It was concluded that the 3D reconstruction of MSCTA for CRC patients before surgery was helpful to understand the location of colorectal tumors, the anatomical structure of mesenteric blood vessels, and their variations. It had a good effect on guiding the implementation of laparoscopic CRC radical resection.

5. Conclusion

The conventional MRI technique and the 3D image reconstructed by MRI based on deep learning were compared in the research in the preoperative evaluation of CRC. Through the comparative analysis of the study results, in terms of consistency with the surgical plane, the assessment results of the experimental group were more consistent than those of the control group and direct observation under laparoscopy, and the difference was remarkable ($P < 0.05$). In terms of tumor T staging, the consistency between the experimental group and pathological biopsy results was higher than that of the control group, and the difference was great ($P < 0.05$).

This research was a small-scale pathological study, and it was not very representative. However, from the results, deep learning-based MRI technology still had certain significance in the application of the preoperative evaluation of CRC. In the long term, the application of this technique in the surgical treatment of other malignant tumors will also obtain good development.

Data Availability

No data were used to support this study.

Conflicts of Interest

The authors declare that they have no conflicts of interest.

References

[1] E. Dekker, P. J. Tanis, J. L. A. Vleugels, P. M. Kasi, and M. B. Wallace, "Colorectal cancer," *The Lancet*, vol. 394, no. 10207, pp. 1467–1480, 2019.

[2] M. Navarro, A. Nicolas, A. Ferrandez, and A. Lanas, "Colorectal cancer population screening programs worldwide in 2016: an update," *World Journal of Gastroenterology*, vol. 23, no. 20, pp. 3632–3642, 2017.

[3] A. Vignali, U. Elmore, M. Milone, and R. Rosati, "Transanal total mesorectal excision (TaTME): current status and future perspectives," *Updates in Surgery*, vol. 71, no. 1, pp. 29–37, 2019.

[4] X. Ni, D. Jia, Y. Chen, L. Wang, and J. Suo, "Is the enhanced recovery after surgery (eras) program effective and safe in laparoscopic colorectal cancer surgery? A meta-analysis of randomized controlled trials," *Journal of Gastrointestinal Surgery*, vol. 23, no. 7, pp. 1502–1512, 2019.

[5] S. Sheng, T. Zhao, and X. Wang, "Comparison of robot-assisted surgery, laparoscopic-assisted surgery, and open surgery for the treatment of colorectal cancer," *Medicine*, vol. 97, no. 34, Article ID e11817, 2018.

[6] A. A. Damadi, E. A. Lax, L. Smithson, and R. D. Pearlman, "Comparison of therapeutic benefit of bupivacaine HCl transversus abdominis plane (tap) block as part of an enhanced recovery pathway *versus* traditional oral and intravenous pain control after minimally invasive colorectal surgery: a prospective, randomized, double-blind trial," *The American Surgeon*, vol. 85, no. 12, pp. 1363–1368, 2019.

[7] H. Shinohara, Y. Kurahashi, S. Haruta, Y. Ishida, and M. Sasako, "Universalization of the operative strategy by systematic mesogastric excision for stomach cancer with that for total mesorectal excision and complete mesocolic excision colorectal counterparts," *Annals of Gastroenterological Surgery*, vol. 2, no. 1, pp. 28–36, 2017.

[8] N. Horvat, C. Carlos Tavares Rocha, B. Clemente Oliveira, I. Petkovska, and M. J. Gollub, "MRI of rectal cancer: tumor staging, imaging techniques, and management," *RadioGraphics*, vol. 39, no. 2, pp. 367–387, 2019.

[9] A. Miles, S. A. Taylor, S. A. Taylor et al., "Patient preferences for whole-body MRI or conventional staging pathways in lung and colorectal cancer: a discrete choice experiment," *European Radiology*, vol. 29, no. 7, pp. 3889–3900, 2019.

[10] A. B. Benson, A. P. Venook, M. M. Al-Hawary et al., "Rectal cancer, version 2.2018, NCCN clinical practice guidelines in oncology," *Journal of the National Comprehensive Cancer Network*, vol. 16, no. 7, pp. 874–901, 2018.

[11] Q. Chen, X. Shuai, and L. Chen, "[Safety and feasibility of the combined medial and caudal approach in laparoscopic D3 lymphadenectomy plus complete mesocolic excision for right hemicolectomy in the treatment of right hemicolon cancer complicated with incomplete ileus]," *Zhonghua Wei Chang Wai Ke Za Zhi*, vol. 21, no. 9, pp. 1039–1044, 2018.

[12] R. R. Bahadoer, E. A. Dijkstra, and B van Etten, "RAPIDO collaborative investigators. Short-course radiotherapy followed by chemotherapy before total mesorectal excision (TME) versus preoperative chemoradiotherapy, TME, and optional adjuvant chemotherapy in locally advanced rectal cancer (RAPIDO): a randomised, open-label, phase 3 trial," *The Lancet Oncology*, vol. 22, no. 1, pp. 29–42, 2021 Jan, Epub 2020 Dec 7. Erratum in: Lancet Oncol. 2021;22(2):e42.

[13] K. F. Birbeck, C. P. Macklin, N. J. Tiffin et al., "Rates of circumferential resection margin involvement vary between surgeons and predict outcomes in rectal cancer surgery," *Annals of Surgery*, vol. 235, no. 4, pp. 449–457, 2002.

[14] W. J. Jeong, B. J. Choi, and S. C. Lee, "Pure natural orifice transluminal endoscopic surgery for rectal cancer: Ta-TME and CME without abdominal assistance," *Asian Journal of Surgery*, vol. 42, no. 2, pp. 450–457, 2019.

[15] F. H. Koh and K.-K. Tan, "Complete mesocolic excision for colon cancer: is it worth it?" *Journal of Gastrointestinal Oncology*, vol. 10, no. 6, pp. 1215–1221, 2019.

[16] C. Riola-Parada, L. García-Cañamaque, V. Pérez-Dueñas, M. Garcerant-Tafur, and J. L. Carreras-Delgado, "Simultaneous PET/MRI vs. PET/CT in oncology. A systematic review," *Revista Española de Medicina Nuclear e Imagen Molecular*, vol. 35, no. 5, pp. 306–312, 2016.

[17] A. C. Tsili, G. Alexiou, C. Naka, and M. I. Argyropoulou, "Imaging of colorectal cancer liver metastases using contrast-enhanced US, multidetector CT, MRI, and FDG PET/CT: a meta-analysis," *Acta Radiologica*, vol. 62, no. 3, pp. 302–312, 2021.

[18] I. B. Guney, Z. Teke, K. A. Kucuker, and O. Yalav, "A prospective comparative study of contrast-enhanced CT, contrast-enhanced MRI and 18F-FDG PET/CT in the preoperative staging of colorectal cancer patients," *Annali Italiani di Chirurgia*, vol. 91, pp. 658–667, 2020.

[19] J. L. Zhang, X. C. Guo, J Liu et al., "[Preoperative evaluation using multi-slice spiral CT angiography of right-side colon vascular in laparoscopic radical operation for right colon cancer]," *Zhonghua Wai Ke Za Zhi*, vol. 57, no. 12, pp. 927–933, 2019, Chinese.

[20] L. Bian, D. Wu, Y. Chen et al., "Clinical value of multi-slice spiral CT angiography, colon imaging, and image fusion in the preoperative evaluation of laparoscopic complete mesocolic excision for right colon cancer: a prospective randomized trial," *Journal of Gastrointestinal Surgery*, vol. 24, no. 12, pp. 2822–2828, 2020.